

43<sup>rd</sup> Annual Symposium of the Ultrasonic Industry Association, UIA Symposium 2014

## Advanced bode plot techniques for ultrasonic transducers

D. A. DeAngelis and G. W. Schulze

*Mechanical Engineering, Ultrasonics Group, Kulicke & Soffa Industries, 1005 Virginia Drive, Fort Washington, PA 19034, USA*

---

### Abstract

The Bode plot, displayed as either impedance or admittance versus frequency, is the most basic test used by ultrasonic transducer designers. With simplicity and ease-of-use, Bode plots are ideal for baseline comparisons such as spacing of parasitic modes or impedance, but quite often the subtleties that manifest as poor process control are hard to interpret or are nonexistent. In-process testing of transducers is time consuming for quantifying statistical aberrations, and assessments made indirectly via the workpiece are difficult. This research investigates the use of advanced Bode plot techniques to compare ultrasonic transducers with known “good” and known “bad” process performance, with the goal of a-priori process assessment. These advanced techniques expand from the basic constant voltage versus frequency sweep to include constant current and constant velocity interrogated locally on transducer or tool; they also include up and down directional frequency sweeps to quantify hysteresis effects like jumping and dropping phenomena. The investigation focuses solely on the common PZT8 piezoelectric material used with welding transducers for semiconductor wire bonding. Several metrics are investigated such as impedance, displacement/current gain, velocity/current gain, displacement/voltage gain and velocity/voltage gain. The experimental and theoretical research methods include Bode plots, admittance loops, laser vibrometry and coupled-field finite element analysis.

© 2015 The Authors. Published by Elsevier B.V. This is an open access article under the CC BY-NC-ND license

(<http://creativecommons.org/licenses/by-nc-nd/4.0/>).

Peer-review under responsibility of the Ultrasonic Industry Association

**Keywords:** Ultrasonic transducer; Wire bonding; Bode plots; Piezoelectric; PZT8; Vibrometer; Coupled-field FEA; ANSYS

---

### 1. Introduction

The Bode plot, displayed as impedance or admittance versus frequency, is the most basic test used by ultrasonic transducer designers. With simplicity and ease-of-use, Bode plots are ideal for baseline comparisons such as spacing of parasitic modes and impedance. But, quite often the subtleties that manifest as poor process control are hard to interpret or are nonexistent from standard Bode plots. In-process testing of transducers is time consuming for quantifying statistical aberrations, and assessments made indirectly via the workpiece are difficult for identifying

cause and effect relationships. Transducer modal surveys require an expensive scanning laser vibrometer and interpretation is esoteric. Advanced bode plot techniques are needed for a-priori process assessment of ultrasonic transducers.

## 2. Specific transducer application

Kulicke & Soffa Industries is the leading manufacturer of semiconductor wire bonding equipment. This “back-end” type of equipment provides ultrasonically welded interconnect wires between the wafer level semiconductor circuitry (die) and the mounting package (frame) as shown in Fig. 1. The ultrasonic transducer delivers energy to a capillary tool for welding tiny gold or copper wires, typically on the order of .001 inches in diameter. Fig. 2 shows the primary steps of the wire bond cycle used to produce the interconnect wires, and how the ultrasonic energy from the transducer is delivered in a “scrubbing motion” to make the welded bonds. Fig. 1(d) shows the on-machine configuration. The single-piece construction “Unibody” transducer uses four diced, rectangular PZT8 piezoceramics, and is ideal for research studies (DeAngelis et al., 2006, 2009, 2010). Portability across 100’s of machines is required for the same customer device in production operations.

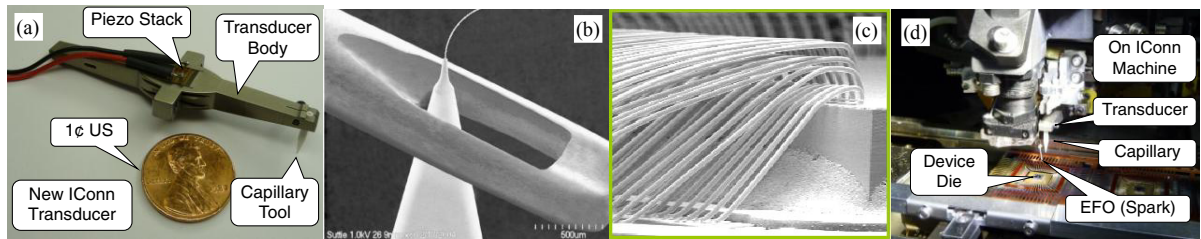


Fig. 1. (a) K&S “Unibody” ultrasonic transducer, (b) Ceramic capillary tool tip with fine gold wire compared to sewing needle, (c) Actual wire bonds from multi-tier package, (d) On-machine configuration of “Unibody” transducer during device wire bonding.

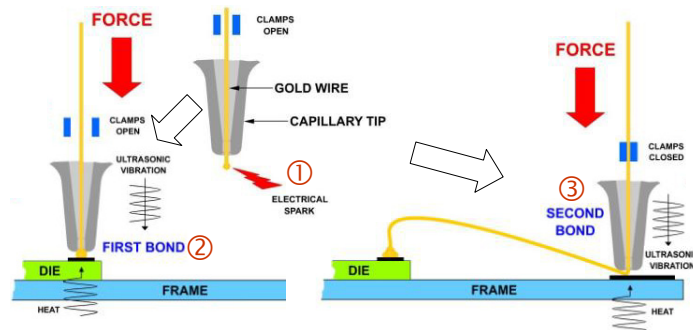


Fig 2. Primary steps 1, 2 and 3 of the wire bond cycle

## 3. Assessment methodology

What aspects of transducer performance are important for ideal process control (Stansfield, 1991, Wilson, 1991, Sherman et al., 2007, Uchino et al., 2003)? The mechanical interfaces must behave linearly in vicinity of the operating mode, such that there is no separation or “gapping” with drive level or frequency change (DeAngelis et al., 2009, 2010); the critical interfaces are tool-to-clamp and the piezoceramic stack. The displacement gain of all surfaces must behave linearly in vicinity of the operating mode and proportional to drive level: the displacement/current gain should be linear in vicinity of resonance, and the displacement/voltage gain should be linear in vicinity of antiresonance (DeAngelis et al., 2006). The tool motions must be consistent in all directions above and below the operating mode: in-plane motions remain in-plane, and linear motions remain linear and in same direction. No local parasitic resonances should be competing with the operating mode; parasitic coupling has a 180° phase change when driven through the operating mode. The usual suspects are shim electrodes, tool clamps, screws and tools. Shim electrode resonances are hard to detect since their manifestation can vary wildly with slight

## 4. Research summary

## 5. Experimental methods and metrics

Figure 1 consists of six photographs arranged in a 2x3 grid, each showing a different component being aligned with a laser dot. Each photograph includes a 3D coordinate system (X, Y, Z) and a callout for the 'Laser Dot'.

- Top or Tip of Tool in X Direction:** Shows a tool tip being aligned with a laser dot. The callout points to the 'Laser Dot (X-Top)' and 'Laser Dot (X-Tip)'.
- Top or Tip of Tool in -Y Direction (Operating Mode Direction):** Shows a tool tip being aligned with a laser dot. The callout points to the 'Laser Dot (Y-Top)' and 'Laser Dot (Y-Tip)'.
- Tip of Tool in Z Direction:** Shows a tool tip being aligned with a laser dot. The callout points to the 'Laser Dot (Z-Tip)'.
- Tool Clamp in -X Direction:** Shows a tool clamp being aligned with a laser dot. The callout points to the 'Laser Dot (X-Clamp)'.
- Piezo Stack in Z Direction:** Shows a piezo stack being aligned with a laser dot. The callout points to the 'Laser Dot (Z-Stack)'.
- Shim Electrode in -Y Direction:** Shows a shim electrode being aligned with a laser dot. The callout points to the 'Laser Dot (Y-Shim)'.

Fig. 4. Methodology for velocity interrogation.

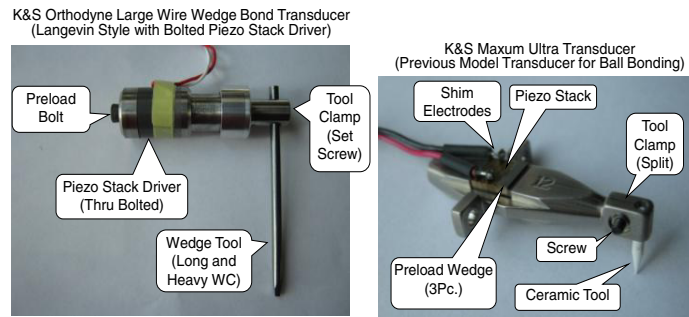


Fig 5. Velocity interrogation target areas for typical transducers.

## 6. Finite element modeling

Fig. 6 shows the piezoelectric coupled-field finite element model from the ANSYS software with coupling via “stiffness” matrix which includes the piezoelectric properties for PZT8 material. The nodes have structural (X, Y, Z displacements) and electric (volt) degrees of freedom. The linear model was created without interface gapping (i.e., no gap elements) to correlate to the “good” transducer, and a constant damping ratio of 0.2% was used for all materials. The forced response was generated using a sine-sweep voltage input to the piezoceramic stack. Fig. 7 shows the FEA derived Bode results for clamp and top of capillary tool in the X-Clamp, X-Top and Y-Top directions as shown in Fig. 4; there is no hysteresis with the linear model, so results are independent of sweep direction. Fig. 8 shows the FEA derived gain ratio results for these same directions. The current and velocity gains are the same with a FEA linear model.

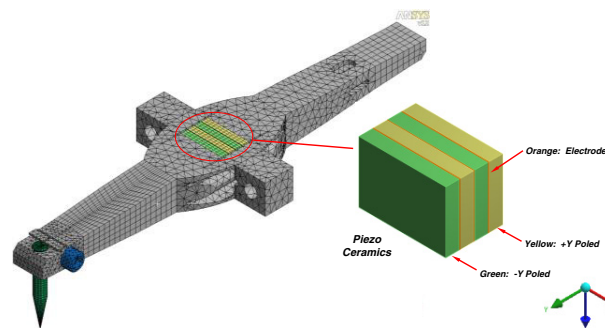


Fig. 6. Piezoelectric coupled-field finite element model in ANSYS software.

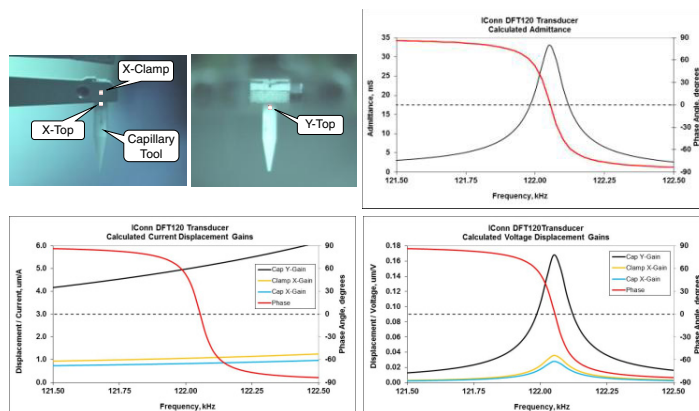


Fig. 7. FEA derived Bode results for clamp and top of capillary.

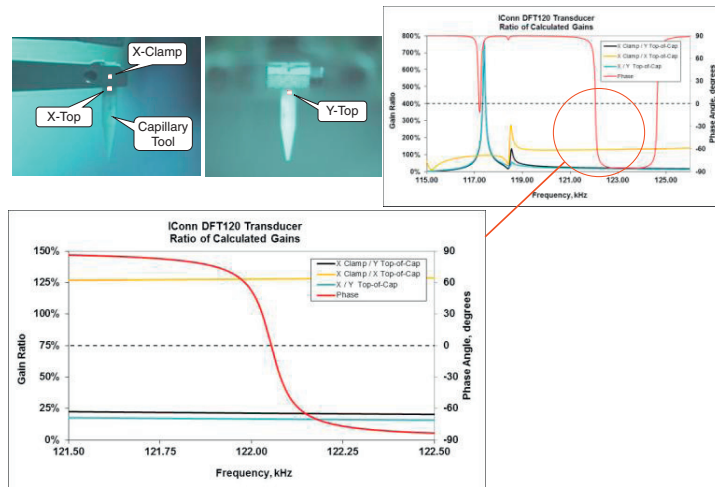


Fig. 8. FEA derived gain ratio results for clamp and top of capillary.

## 7. Experimental results

Figs. 9-12 show the advanced Bode technique results for the “good” transducer with the expected or “good” process response. As shown in Fig. 4, the velocity interrogation locations are X-Clamp, X-Top and Y-Top. The gain ratio results presented in Fig. 12 are for comparison to the linear FEA model, to demonstrate that a “good” process response is inherently a linear response. Figs. 13-17 show the advanced Bode technique results for the “bad” transducer with poor process response (i.e., inconsistent shears). The velocity interrogation locations are the same as the “good” transducer.

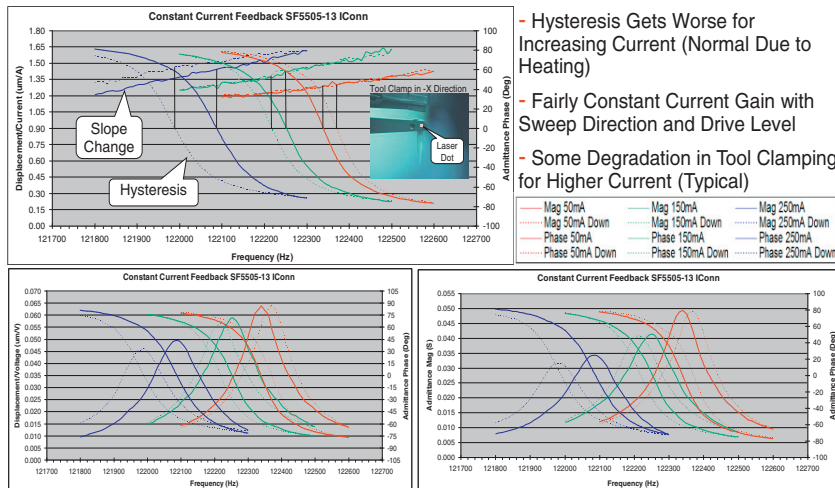


Fig. 9. Constant current Bode for “good” transducer with X-Clamp velocity.



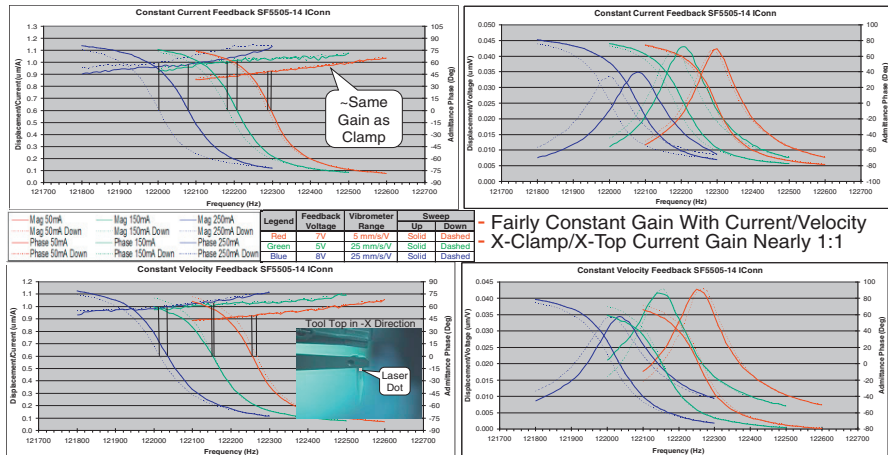


Fig. 10. Constant current/velocity mode for "good" transducer with X-Top velocity.

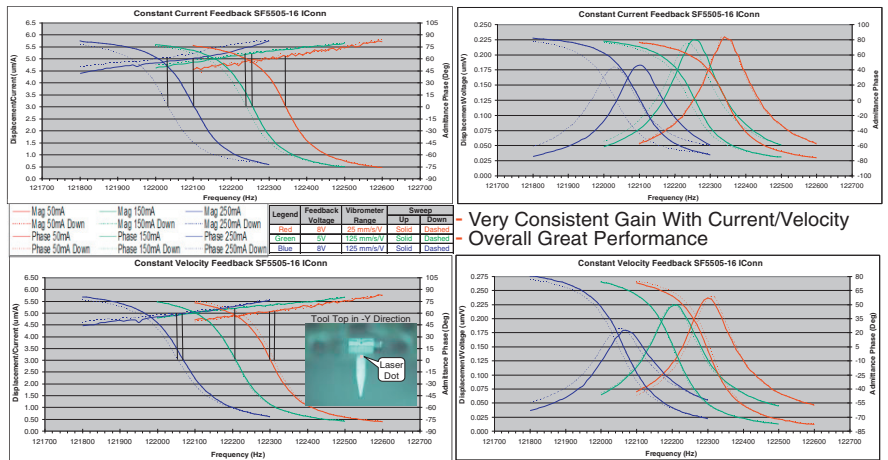


Fig. 11. Constant current/velocity mode for "good" transducer with Y-Top velocity.

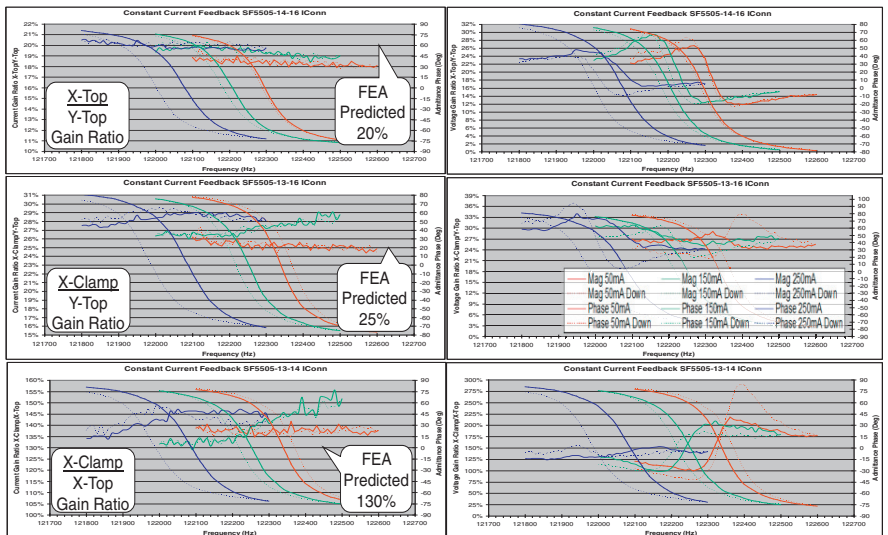


Fig. 12. Gain ratios with X and Y velocities for "good" transducer.

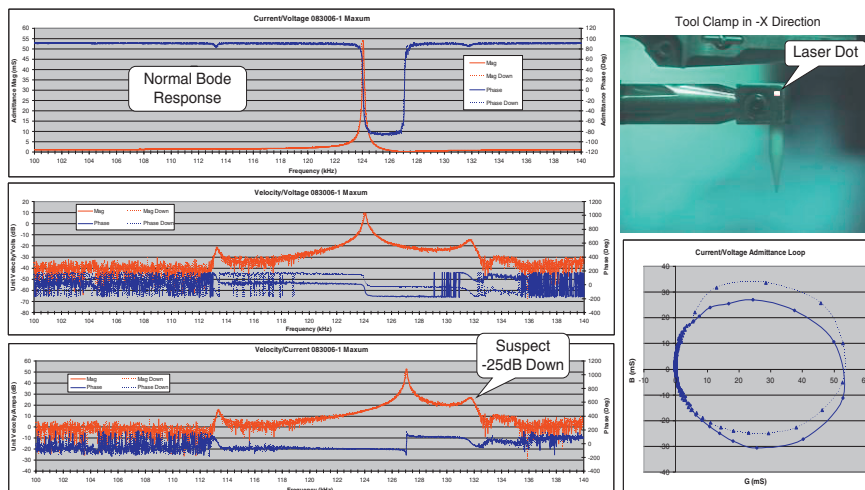


Fig. 13. Standard Bode for “bad” transducer with X-Clamp velocity.

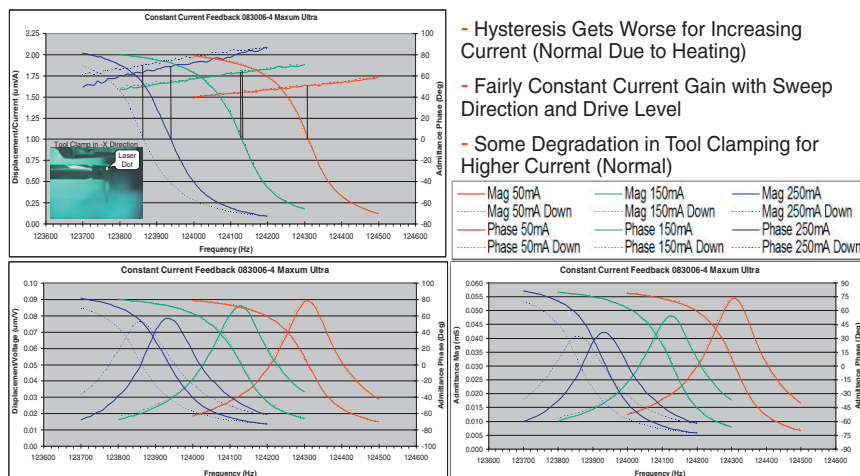


Fig. 14. Constant current Bode for “bad” transducer with X-Clamp velocity.

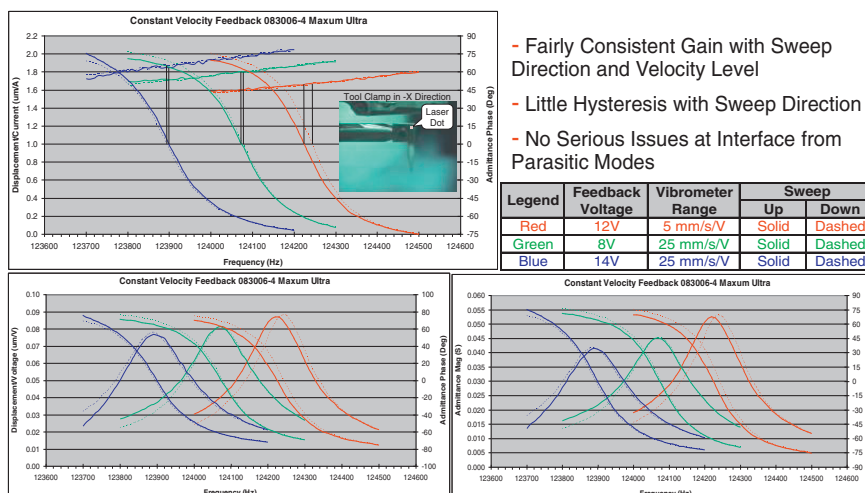


Fig. 15. Constant velocity Bode for “bad” transducer with X-Clamp velocity.

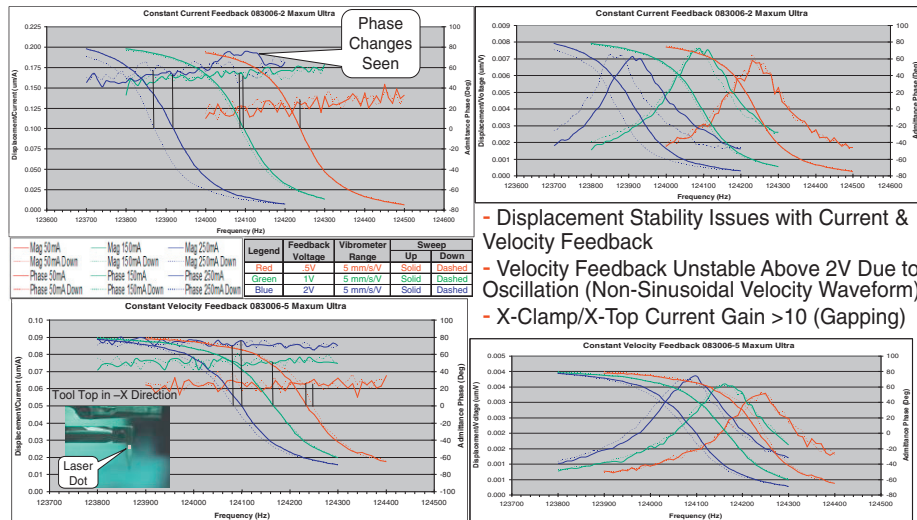


Fig. 16. Constant current/velocity Bode for "bad" transducer with X-Top velocity.

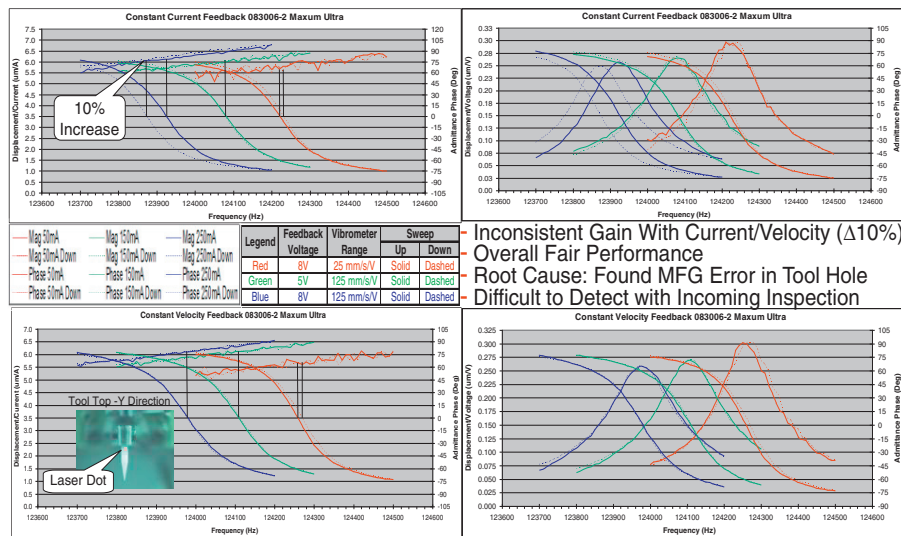


Fig. 17. Constant current/velocity Bodes for "bad" transducer with Y-Top velocity.

## 8. Conclusions

The transducer with "good" process performance conforms to behavior as predicted by the ideal linear FEA model with glued interfaces (i.e., no gap elements). Non-linear behavior in the tool was shown to be the root cause of poor process (i.e., low shear force): manufacturing error exacerbated inherent design problem in the tool clamp. Phase changes from closely spaced parasitic modes can lead to hysteresis effects due to interface gapping as seen from the non-sinusoidal velocity profile; heating effects can also cause hysteresis. Velocity based Bode plots can pick-up subtleties typically overlooked without a full laser vibrometer modal survey. A unique set of interrogation locations and assessment criteria is required for each specific transducer design and process application; wire bonding is inordinately sensitive to tool motions due to delicate balance of forces exerted on tiny ball and micro bond pad structure; inconsistent energy delivery to the tool is a root cause of poor process.



## References

- C. H. Sherman and J. L. Butler, *Transducers and Arrays for Underwater Sound*. New York, NY: Springer Science, 2007.
- D. A. DeAngelis and D. C. Schalcosky, "The Effect of PZT8 Piezoelectric Crystal Aging on Mechanical and Electrical Resonances in Ultrasonic Transducers," 2006 IEEE Ultrasonics Symposium, Session P2O-10.
- D. A. DeAngelis, G. W. Schulze, "Optimizing Piezoelectric Ceramic Thickness in Ultrasonic Transducers," 2010 UIA Symposium Proceedings, IEEE XPloré.
- D. A. DeAngelis, G. W. Schulze, "Optimizing Piezoelectric Crystal Preload in Ultrasonic Transducers," 2009 UIA Symposium Proceedings, IEEE XPloré.
- D. Stansfield, *Underwater Electroacoustic Transducers*. Los Altos, CA: Peninsula Publishing, 1991.
- K. Uchino and J. R. Giniewicz, *Micromechatronics*. New York, NY: Marcel Dekker, 2003.
- M. Umeda, K. Nakamura, S. Takahashi, S. Ueha, "An Analysis of Jumping and Dropping Phenomena of Piezoelectric Transducers using the Electrical Equivalent Circuit Constants at High Vibration Amplitude Levels," *Japanese Journal of Applied Physics* Vol. 39 (2000) pp. 5623-5628.
- O. B. Wilson, *Introduction to Theory and Design of Sonar Transducers*. Los Altos, CA: Peninsula Publishing, 1991.
- S. O. Ural, S. Tuncdemir, Y. Zhuang, K. Uchino, "Development of a High Power Piezoelectric Characterization System and Its Application for Resonance/Antiresonance Mode Characterization," *Japanese Journal of Applied Physics* 48 (2009) 056509.